Kays, W. M., and A. L. London, "Compact Heat Exchangers," 2nd ed., McGraw-Hill (1964).
Mills, A. A., and F. W. Steffgen, "Catalytic Methanation," *Catalysis Reviews*, **8**, 2, (159–210) (1973).
Parent, Y., "The Annular Heat Pipe Operating Limit Equations and Chemical Reactor Application," Ph.D. Thesis, Lehigh University (1980).
Parent, Y. O., R. W. Coughlin and H. S. Caram, "Operational Limits for the Annular Heat Pipe," in preparation.
Peters, H., "Catalytic Reactor Tube Liner," U. S. Patent 3,353,923, (1967).
Rase, H. F., "Chemical Reactor Design for Process Plants," **1-2**, Wiley (1977).
Smith, J. M., "Chemical Engineering Kinetics," 2nd ed., McGraw-Hill (1970).
Smith, T. G., and J. J. Carberry, "Design and Optimization of a Tube-Wall Reactor," *Chem. Eng. Sci.*, **30**, 2, (221–227) (1975).
Tallmadge, J. A., "Packed Bed Pressure Drop—An Extension to Higher Reynolds Numbers," *AIChE J.*, **16**, 1092 (1970).

Manuscript received April 27, 1981; revision received February 23, and accepted June 18, 1982.

Combustion of Carbon Residue from Oil Shale Retorting

The combustion of a bed of particles impregnated with carbon is considered. An analysis is developed for the combustion wave after it has progressed some distance into the bed. It is shown that the calculations are considerably simplified by choosing a coordinate system that moves with the combustion wave and by neglecting dispersion of heat or mass.

MILTIADIS HISKAKIS and T. J. HANRATTY

Department of Chemical Engineering
University of Illinois
Urbana, IL 61801

SCOPE

In the combustion retorting of oil shale, a combustion wave is caused to move down through a bed of raw shale particles. Hot inert gases flow ahead of the wave and decompose the kerogen in the raw shale. Oil produced by this pyrolysis reaction is carried from the hot zone as a vapor, which condenses on cold shale particles and falls out the bottom of the bed as a liquid product. The pyrolysis of the kerogen leaves behind a carbon residue which provides the fuel for the combustion. The size of the oil yield from the process depends on keeping the combustion zone separated from the retorting zone and on minimizing the combustion of oil by oxygen which has bypassed the hot carbon residue.

We have been exploring a model of this process which solves the balance and rate equations in a coordinate system which moves with the combustion zone. Considerable simplifications of the equations are realized by neglecting dispersion of heat and mass in the flow direction and by assuming an adiabatic process. Our first step in implementing this model has been to consider the combustion of a bed of particles impregnated with carbon.

For large enough times, the combustion wave in a bed of burning carbon can reach a fully developed condition where the velocity, the temperature and the composition profiles do not change with time. This paper presents an analysis of this fully developed zone.

CONCLUSIONS AND SIGNIFICANCE

A modification of the general theoretical model of Baer and Dahl (1980) is used. In their analysis it is assumed that one percent of the oxygen in the inlet gas escapes unburned and that all of the carbon is consumed. It is shown that this assumption is not correct. In fact the calculation of the conversion of oxygen or of carbon emerges as the principle theoretical problem. Methods for calculating the effect of operating variables on the breakthrough of oxygen or of carbon are developed.

The errors involved in neglecting the influence of the dispersion of heat and of oxygen are explored. It is shown that these effects can be neglected provided the heat transfer coefficient between the gas and the solid is adjusted.

INTRODUCTION

The analysis uses separate heat balance equations for the gas and the solid and a shrinking core model for the carbon combustion. A parameter

$$\beta = \frac{\frac{\dot{m}_g}{A} C_g}{V \rho_s C_s (1 - \epsilon)}$$

is critically important.

The condition $\beta \neq 1$ is necessary for the existence of a fully developed temperature wave (Baer and Dahl, 1980).

For $\beta < 1$, the combustion occurs at the front of the thermal wave that moves through the bed. The tail of the wave is an un-

M. Hiskakis is a fellow of the Alexandros Onassis Institute.

steady solid cooling zone in which the cold gas containing oxygen is heated by passing over the inert hot shale that remains after combustion. The velocity of this cooling zone is less than the velocity of the combustion zone so that there is a region of hot burned particles which increases in size as the wave progresses into the bed.

For $\beta > 1$, the combustion occurs at the tail end of the wave. The front of the wave then consists of an unsteady solid heating zone that moves at a faster velocity than the combustion zone.

The assumption by Baer and Dahl (1980) that all the carbon is consumed and that one percent of the oxygen escapes unburned requires the kinetics of the combustion be ignored. In the work described in this paper two methods for modeling the combustion of carbon are considered: In one of these an autoignition of carbon is assumed to occur at a fixed temperature. In the other, a kinetic model for the combustion of carbon is used. Small changes in the temperature profile are found to have a strong effect on the breakthrough of oxygen or of carbon.

Most of the characteristics of the thermal wave can be calculated from simple algebraic equations provided the oxygen or carbon breakthrough are known. Consequently, the prediction of the breakthrough emerges as the principle theoretical problem.

OUTLINE OF THE MODEL

A fully developed thermal wave moving through the bed of carbon is pictured as having the structure shown in Figure 1 for $\beta < 1$.

In Zone I, hot burned shale heats up the cold gas entering the bed. Zone II is the combustion region in which the reaction between the oxygen and the carbon takes place. In Zone III hot gas emerging from the combustion zone heats up raw cold shale to the ignition temperature.

It is assumed (Sohn and Kim, 1980; Mallon and Braun, 1976; Thomson, 1981; Soni and Thomson, 1979; Yoon et al., 1978) that the reaction between the carbon and oxygen that takes place during the char combustion is

$$C + O_2 \rightarrow CO_2 \qquad (1)$$

At higher temperature and in the presence of a large amount of CO_2 produced by the char combustion and the carbonate decomposition the following reaction can occur

$$C + CO_2 \rightarrow 2CO$$

For simplicity we assumed, as did Fausett (1975) and Baer and Dahl (1980) that the only reaction that occurs is Eq. 1.

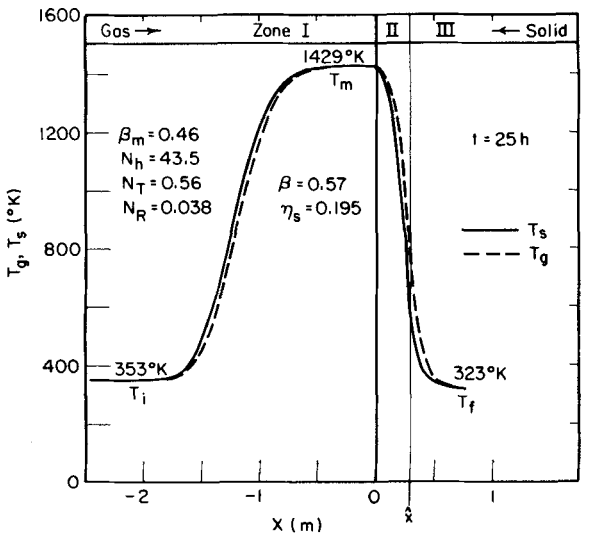

Figure 1. Temperature profile for a plug-flow carbon-bed combustion with $\beta < 1$.

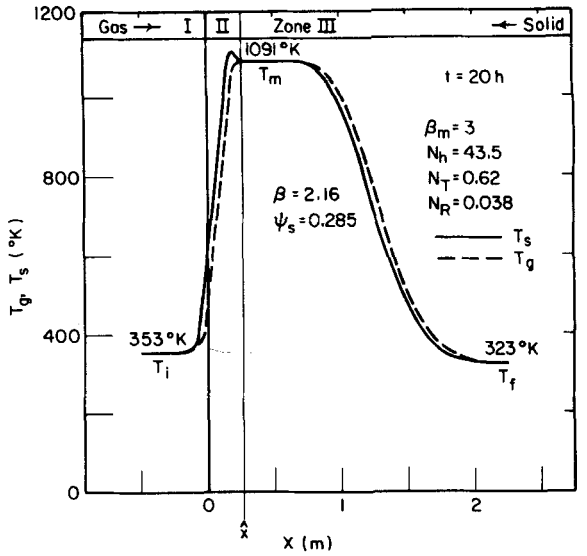

Figure 2. Temperature profile for a plug-flow carbon-bed combustion with $\beta > 1$.

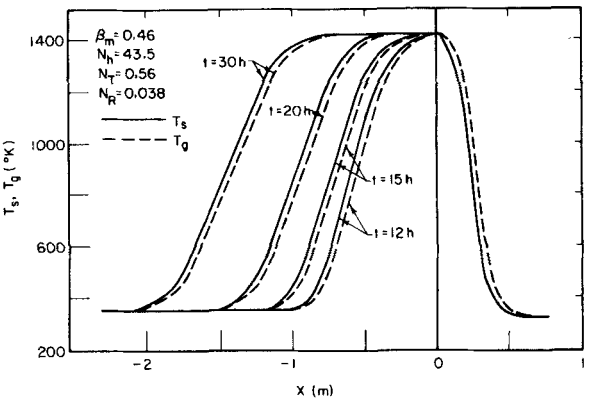

Figure 3. Evolution of the temperature profile with time.

From an overall mass balance the following equation is developed to describe the velocity with which the combustion zone moves through the bed:

$$V = \frac{3N_o \frac{\dot{m}_g}{A}(1 - \eta_s)}{8\rho_s \chi_s (1 - \epsilon)(1 - \Psi_s)} \qquad (2)$$

Here η_s and Ψ_s are the fractions of initial oxygen and carbon remaining after combustion.

From an overall heat balance it is found that the thermal wave in Zone I moves with a velocity

$$V_{us} = \beta V \qquad (3)$$

For $\beta < 1$, or $V_{us} < V$ a plateau region exists between Zones I and II, which increases in length at a rate given by $(1 - \beta)V$, Figure 3.

The case of $\beta > 1$ is depicted in Figure 2. In this case, the combustion Zone II is located just behind the thermal plateau and the thermal region, Zone III, in the front of the plateau moves with a velocity given by Eq. 3. Consequently, the plateau lengthens at a rate given by $(\beta - 1)V$.

The following heat balance equations are used to describe the temperature profile in the gas and in the solid phase:

$$\rho_g \epsilon C_g \frac{\partial T_g}{\partial t} = h_{gs} a_p (1 - \epsilon)(T_s - T_g) - \frac{\dot{m}_g}{A} C_g \frac{\partial T_g}{\partial z} \qquad (4)$$

$$\rho_s (1 - \epsilon) C_s \frac{\partial T_s}{\partial t} = -h_{gs} a_p (1 - \epsilon)(T_s - T_g) - \Delta H r (1 - \epsilon) \qquad (5)$$

It is to be noted that fluid properties have been assumed constant and that heat dispersion has been neglected.

Because of the large change of temperature the assumption of constant ρ_g is not a good approximation. However, the errors arising in the evaluation of $\rho_g \epsilon C_g \partial T_g/\partial t$ are of little consequence since this term is small compared to $(\dot{m}_g/A)\, C_g\, \partial T_g/\partial z$; i.e., the thermal wave velocity is small compared to the gas velocity. One can also expect changes in $\dot{m}_g$, and, therefore, h_{gs}, because of the consumption of carbon by gas through the combustion process. The effect of these changes is difficult to estimate because of uncertainties in the prediction of h_{gs}.

The heat balance Eqs. 4 and 5 can be changed to ordinary differential equations if it is assumed that the temperature profiles are steady in a coordinate system moving with velocity V. The balance Eqs. 4 and 5 then become

$$-\frac{\dot{m}_g}{A} C_g \frac{dT_g}{dx} + h_{gs} a_p (1-\epsilon)(T_s - T_g) = 0 \tag{6}$$

$$V \rho_s C_s (1-\epsilon) \frac{dT_s}{dx} - h_{gs} a_p (1-\epsilon)(T_s - T_g) - \Delta H r (1-\epsilon) = 0 \tag{7}$$

In this framework, one is considering a bed of solids moving counter-currently, with velocity V, to a gas flow. Because the velocity V is very small compared to $\dot{m}_g$, we assume the gas flow rate relative to the moving frame is equal to the gas flow rate relative to the stationary bed.

SOLUTIONS OF HEAT BALANCE EQUATIONS WITHOUT REACTION

Steady-State Thermal Waves

It is of interest first to consider the solution of Eqs. 6 and 7 for thermal Zones I and III, where $r = 0$. One gets

$$T_g = P + S \exp(-\alpha x) \tag{8}$$

$$T_s = P + S\beta \exp(-\alpha x) \tag{9}$$

where P and S are arbitrary constants and α and β are defined by the equations

$$\alpha = (1-\beta) \frac{h_{gs} a_p (1-\epsilon)}{\frac{\dot{m}_g}{A} C_g} \tag{10}$$

$$\beta = \frac{\frac{\dot{m}_g}{A} C_g}{V \rho_s C_s (1-\epsilon)} \tag{11}$$

From Eq. 10, it is seen that if $\beta < 1$ parameter α is positive and $T_g > T_s$. For $\beta > 1$ parameter α is negative and $T_s > T_g$. As pointed out by Baer and Dahl (1980), the above results indicate that a steady-state solution is not possible for both Zones I and III.

For $\beta > 1$ the steady state solution predicts a zone of exponentially increasing temperature where the gas is being heated by the solid. We conclude that, for this case, Zone I is a steady state thermal wave.

It is of interest to compare Eqs. 8 and 9 with the solution of the temperature balance equation presented by Fausett (1975). The temperatures of the gas and the solid are assumed equal. The steady state balance can then be written as

$$\left(V C_s \rho_s (1-\epsilon) - \frac{\dot{m}_g}{A} C_g \right) \frac{dT}{dx} = K \frac{d^2 T}{dx^2} \tag{12}$$

where K is the effective dispersion coefficient and r has been assumed to be zero. The solution of this equation is of the same form as the solution of Eqs. 6 and 7 where $T = (T_s + T_g)/2$ and $r = 0$, if the dispersion coefficient K is redefined as

$$K = \frac{\dot{m}_g}{A} C_g \frac{V \rho_s C_s}{h_{gs} a_p} \tag{13}$$

It is therefore seen that the two equation model Eqs. 6 and 7 includes effects that are the same as the dispersion term that is needed in the one equation model (Eq. 12). This opens the possibility, which will be explored later, that an alteration of the h_{gs} term in Eqs. 6 and 7 would have the same effect as including dispersion terms.

Unsteady-State Thermal Waves

From the arguments presented in the previous section, we conclude that Zone I for $\beta < 1$ and Zone III for $\beta > 1$ are to be described by an unsteady thermal wave moving with a velocity V_{us} given by Eq. 3. For the first case, an unsteady cooling of a hot bed of solids of temperature T_m is accomplished with an incoming cold gas of temperature T_i. The cooling proceeds until at a sufficient distance downstream, the temperature of the solid and the gas are equal. As time passes the solid at the entry section is cooled down to the gas temperature.

The equations describing the temperatures of the gas and solid are Eqs. 4 and 5 with $r = 0$. These are solved using the boundary conditions

$$\begin{aligned} t = 0 \quad & T_s = T_m \\ & T_g = T_i \\ t > 0 \quad z = 0 \quad & T_g = T_i \\ z = \infty \quad & T_s = T_m \end{aligned}$$

After a sufficiently long period of time a condition is reached where at $z = 0$, $T_s = T_g = T_i$ and at $z = V_{us} t$, $T_s = T_g = T_m$. This problem is the same as that of a semi-infinite bed of solids at a temperature T_m being heated up or cooled down by a gas at a temperature T_i over the length interval $z = 0$ to $z = V_{us} t$. An analytical solution of this system is presented by Carslaw and Jaeger (1959) and a graphical solution by Hougen and Marshall (1947). A numerical solution based on the graphical one is used in our calculations.

The Zone III, temperature profiles for $\beta > 1$ are pictured as given by the large time, t, solution for the heating of a cold bed of length $z = V_{us} t$, of particles of temperature T_f with a hot gas temperature T_m.

For $\beta < 1$, the long time unsteady solution for Zone I is matched to a steady state combustion zone moving through the bed with velocity V. At the upstream end of the combustion zone the gas and solid temperatures are equal to the temperature T_m defined in the unsteady-state solution. For $\beta > 1$, the Zone III long time unsteady solution is matched at its upstream end to a steady-state combustion zone. At the matching point, the gas and solid temperature are equal to T_m.

STEADY-STATE COMBUSTION WAVES

Solution Using First-Order Rate Equation

The steady-state combustion wave is described as a solution of Eqs. 6 and 7 with $r \neq 0$. The rate of consumption of carbon, r, is described by a first-order equation with respect to oxygen concentration. If it is assumed that the particles are spheres of radius R_p homogeneously impregnated with carbon, the following expression gives the rate for carbon consumption:

$$r = \frac{9 N_o \rho_g}{8 R_p} \frac{\eta}{\frac{R_p(\Psi^{-1/3} - 1)}{D_e} + \frac{3 \rho_g N_o \Psi^{-2/3}}{8 X_s \rho_s R_p A_1 e^{-E/RT_s}} + \frac{1}{K_g}} \tag{14}$$

Strictly, Eq. 4 is valid only for the reaction of a nonporous solid in which chemical reaction takes place at the sharp interface between the nonporous reacted core and the porous ash layer. Justification for using Eq. 14 to approximate combustion in porous spent shale is obtained if it is assumed that the law of additive reaction times for a nucleation and growth model is applicable (Sohn, 1979).

The third term in the denominator of Eq. 14 represents the

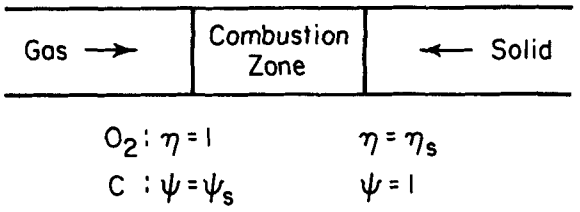

Figure 4. Combustion zone without oxygen diffusion.

gas-phase resistance on the outside of the particle and the mass transfer coefficient K_g can be estimated from an extrapolation of the correlation given by DeAcetis and Thodos (1960). The term K_g is assumed constant. The calculations show that the value of K_g does not have an appreciable effect on the results, since the reaction rate is controlled by the diffusion of oxygen through the gas film surrounding the particle for a negligible amount of time. The first term gives the resistance that results because the oxygen must diffuse through the burned part of the shale particle in order to reach the unburned carbon. The variable $(\Psi^{-1/3} - 1)$ indicates the increase of the diffusion path as the carbon is consumed. The effective diffusion coefficient D_e was determined experimentally by Mallon and Braun (1976). The second term gives the resistance due to reaction. Kinetic parameters for the combustion of carbon are given in papers by Yoon et al. (1978), Soni and Thomson (1979), and Sohn and Kim (1980).

The rate of carbon consumption can be expressed entirely in terms of the carbon concentration by developing an algebraic equation between Ψ and η. If the properties are assumed constant and oxygen diffusion is ignored the following mass balances can be written for the oxygen and the carbon:

$$\frac{\dot{m}_g}{A}\frac{d\eta}{dx} + \frac{1-\epsilon}{N_o} r_{O_2} = 0 \tag{15}$$

$$V\rho_s\chi_s\frac{d\Psi}{dx} - r = 0 \tag{16}$$

From the stoichiometry of the reaction, Eq. 1, it follows that

$$\frac{r}{12} = \frac{r_{O_2}}{32} \tag{17}$$

The boundary conditions for the combustion zone are given in Figure 4. By combining these conditions with Eqs. 15, 16 and 17 the following linear relation between the oxygen and carbon concentrations is obtained:

$$\eta = \frac{1 - \eta_s\Psi_s - (1-\eta_s)\Psi}{1-\Psi_s} \tag{18}$$

The temperature and concentration profiles are calculated by solving simultaneously Eqs. 6, 7, 16, 14 and 18 using the following boundary conditions:

For $\beta < 1$, $x = 0$ $T_s = T_g$: matching the unsteady-state zone

$$T_s = T_m = T_f + \frac{|\Delta H|\chi_s(1-\Psi_s)}{C_s|1-\beta|}$$

$\eta = 1$

$\Psi_s = 0$: no carbon breakthrough

$x = \hat{x}$ $\Psi = 1$

$x \to \infty$ $T_s = T_g = T_f$

For $\beta > 1$, $x = \hat{x}$ $T_s = T_g$: matching the unsteady-state zone

$$T_s = T_m = T_i + \frac{|\Delta H|\chi_s(1-\Psi_s)}{C_s|1-\beta|}$$

$\eta_s = 0$: no oxygen breakthrough

$\Psi = 1$

$x = 0$ $\eta = 1$

$x \to -\infty$ $T_s = T_g = T_i$

These boundary value problems are solved using shooting methods (Carnahan et al., 1976) which give either the oxygen breakthrough, η_s, or the carbon breakthrough, Ψ_s.

The breakthrough occurs because the solid is cooled below the ignition temperature before all the oxygen (for $\beta < 1$) or all the carbon (for $\beta > 1$) has reacted.

Solution Using Auto-Ignition Temperature

Because the temperature varies exponentially in the regions of lower temperature and the rate of combustion increases quite rapidly with temperature, the region in which significant reaction is occurring can be modeled by assuming the rate of reaction is extremely fast compared to the rate of oxygen diffusion (Mallon and Braun, 1976; Docter and Turner, 1978). Consequently the rate of combustion of carbon is given as

$$r = 0 \qquad \text{for } T < T_{sf}$$

$$r = \frac{9N_o\rho_g}{8R_p}\frac{\eta}{\dfrac{R_p(\Psi^{-1/3}-1)}{De} + \dfrac{1}{K_g}} \quad \text{for } T > T_{sf} \tag{19}$$

The specification of an autoignition temperature, T_{sf}, replaces the specification of kinetic parameters A_1 and E.

The advantage of this approach is that Eq. 19 is independent of the details of the temperature profile. This means that the equations for the concentration and temperature variations can be calculated independently.

By combining Eqs. 19, 18 and 16 the following equation can be obtained for the variation of Ψ with x in the combustion zone:

$$x = \frac{V}{C}\left(D + \frac{F}{2N}\right) ln\left(\frac{B - C\Psi}{B - C\Psi_s}\right) - \frac{3VF}{2CN} ln\left(\frac{N + \Psi^{1/3}}{N + \Psi_s^{1/3}}\right) + \\ + \frac{\sqrt{3}VF}{CN}\left\{\tan^{-1}\frac{2\Psi^{1/3} - N}{N\sqrt{3}} - \tan^{-1}\frac{2\Psi_s^{1/3} - N}{N\sqrt{3}}\right\} \tag{20}$$

$$G = -\frac{9DeK_gN_o\rho_g}{8\chi_s\rho_sR_p(1-\Psi_s)} \qquad B = (1-\eta_s\Psi_s)G \qquad C = (1-\eta_s)G$$

$$F = R_pK_g \qquad D = De - F \qquad N = -\sqrt{\frac{B}{C}}$$

By evaluating the position x for which the temperature equals T_{sf} and substituting it into Eq. 20, the breakthrough η_s or ψ_s can be calculated.

Baer and Dahl (1980) assume in their model $\eta_s = 0.01$ and $\Psi_s = 0$ for both $\beta < 1$ and $\beta > 1$ and used an expression similar to Eq. 20 to calculate the concentration profile. They then used this concentration profile to solve for the temperature profile. This does not seem to be a reasonable approach since the auto-ignition temperature is then allowed to vary in an arbitrary manner.

The behavior of the temperature profiles at temperature less than T_{sf} (auto-ignition temperature) is given by Eqs. 8 and 9. The difference in the temperatures of the gas and solid at the matching point between the steady state combustion wave and the steady-state thermal wave can be evaluated by equating the velocities of the two waves. For $\beta < 1$ at $x = \hat{x}, T_s = T_{sf}$

$$T_g - T_{sf} = \frac{1-\beta}{\beta}(T_{sf} - T_f) \tag{21}$$

and for $\beta > 1$ at $x = 0$, $T_s = T_{sf}$

$$T_g - T_{sf} = \frac{\beta - 1}{\beta}(T_{sf} - T_i) \tag{22}$$

For the calculations presented in this paper either η_s or Ψ_s is assumed and Eq. 20 is used to calculate a first approximation for the concentration profile. Equations 6 and 7 are solved for the temperatures using Eqs. 18 and 19 to evaluate r. The calculated temperatures are to satisfy the condition $T_s = T_g$ at one boundary and Eqs. 21 and 22 at the other. If these boundary conditions are not satisfied a new value of η_s or Ψ_s is assumed.

As is evident from Eq. 7 there is a discontinuity in dT_s/dx at the x location where the auto-ignition temperature is reached since here r changes discontinuously from a finite value to zero.

Parameterization of the Problem

For the equations defined above the following relations for η_s and Ψ_s can be defined for the case in which an auto-ignition model is used and dispersion of heat or mass is ignored:

$$\eta_s = f_2\left(\beta_m, N_h, \frac{T_{sf}C_g}{|\Delta H|}, \frac{T_f}{T_{sf}}\right) \tag{23}$$

$$\Psi_s = g_2\left(\beta_m, N_h, \frac{T_{sf}C_g}{|\Delta H|}, \frac{T_i}{T_{sf}}\right) \tag{24}$$

Here β_m is a modified β parameter defined as

$$\beta_m = \frac{8\chi_s C_g}{3N_o C_s} = \beta\left(\frac{1-\eta_s}{1-\Psi_s}\right) \tag{25}$$

This parameter is strongly related to the velocity, V, as can be seen from Eqs. 2 and 11.

The group N_h is given by

$$N_h = \frac{h_{gs}a_p}{\frac{De}{R_p^2}C_g\rho_g} \tag{26}$$

which for a bed of spheres of radius R_p becomes

$$N_h = \frac{3h_{gs}R_p}{D_e C_g \rho_g} \tag{27}$$

Dimensionless groups

$$N_R = \frac{T_{sf}C_g}{|\Delta H|} \tag{28}$$

$$N_T = \frac{T_f}{T_{sf}} \text{ or } \frac{T_i}{T_{sf}} \tag{29}$$

characterize the auto-ignition process.

If a kinetic model for the combustion process is used N_R and N_T are replaced by

$$N_R = \frac{E}{|\Delta H|} \tag{30}$$

$$N_T = \frac{RT_f}{E} \text{ or } \frac{RT_i}{E} \tag{31}$$

so that

$$\eta_s = f_1\left(\beta_m, N_h, \frac{E}{|\Delta H|}, \frac{RT_f}{E}\right) \tag{32}$$

and

$$\Psi_s = g_1\left(\beta_m, N_h, \frac{E}{|\Delta H|}, \frac{RT_i}{E}\right) \tag{33}$$

CALCULATED RESULTS

Temperature Profiles

Experimental studies of shale oil retorts (Campbell and Gregg, 1979) (Braun, 1979) show that β less than unity is the most commonly encountered case.

A calculated temperature profile for $\beta = 0.57$, $N_h = 43.5$, $N_R = 0.038$ and $N_T = 0.56$ is shown in Figure 1. The parameters used in this calculation were taken from Lawrence Livermore Laboratory run S-11 and are summarized in Table 1. The auto-ignition model with a value $T_{sf} = 573$ K (Carley, 1980) was used. The point $x = 0$ represents the beginning of the steady-state combustion zone and $\hat{x}$, the location at which the solid reaches its auto-ignition temperature. At $\hat{x}$ the steady-state combustion zone is matched to a steady-state thermal wave and there is a discontinuity in the derivatives of T_s and T_g.

At $x = 0$ the combustion zone is matched to an unsteady-state cooling zone. As time proceeds this cooling zone increases in size. Figure 3, which illustrates this behavior, shows that the heat generated by the combustion of the carbon appears mainly as a widening of the temperature plateau.

The use of the kinetic model for the combustion of the carbon avoids the occurrence of the discontinuity of the temperature derivatives at $x = \hat{x}$. Calculations using values of $A_1 = 1.79 \times 10^6$ 1/atm·s (6.31×10^7 1/kPa·h) and $E = 27$ kcal/mol (113 kJ/mol) (Yoon et al., 1978), the values of $A_1 = 1.43 \times 10^5$ 1/atm·s (5.08×10^5 1/kPa·h) and E = 23.2 kcal/mol (97.2 kJ/mol) (Soni and Thomson, 1979), or the values of $A_1 = 2.61 \times 10^5$ 1/atm·s (9.26×10^6 1/kPa·h) and E = 22.02 kcal/mol (92.19 kJ/mol) (Sohn and Kim, 1980) are compared with the auto-ignition model in Table 2. We have used the auto-ignition model in most of our calculations because of its simplicity and because of uncertainty regarding the correct values for the kinetic parameters.

Temperature profiles for the case of $\beta = 2.16$, $N_h = 43.5$, $N_R = 0.038$ and $N_T = 0.62$ using the auto-ignition model are shown in Figure 2. The parameters used in the calculation are the same as those used in Figures 1 and 3, except that the bed was assumed to be much richer in carbon ($\chi_s = 0.04$ instead of $\chi_s = 0.021$) and the gas poorer in oxygen ($N_o = 0.06$ instead of $N_o = 0.21$). Steady-state combustion and thermal zones are now located at the rear of the thermal wave. The local maximum that occurs around $x = \hat{x}$ results from the burning of carbon on the surface of the particle in a regime controlled by the diffusion of oxygen through the gas film surrounding the particle.

TABLE 1. VALUES USED FOR OUR CALCULATIONS

Data for retorting run S-11 of the Lawrence Livermore Laboratory presented by Campbell (1979).

ϵ	= 0.47
ρ_g	= 0.44 kg/m^3 (Perry, 1969)
ρ_s	= 1,880 kg/m^3
C_g	= 0.523 kcal/kg·K (2.2 kJ/kg·K) (Perry, 1979)
C_s	= 0.305 kcal/kg·K (1.27 kJ/kg·K)
R_p	= 0.02 m
μ_g	= 0.13 kg/h·m (Shih, 1978)
k_f	= 0.05 kcal/h·m·K (0.2 kJ/h·m·K) (Shih, 1978)
De	= 0.03 m^2/h (Mallon, 1976)
k_g	= 60 m/h (DeAcetis, 1960)
ΔH	= −7,800 kcal/kg·°C (−32,657 kJ/kg·°C) (Perry, 1969)
N_o	= 0.21 (air)
$\frac{\dot{m}_g}{A}$	= 29.42 kg/h·m^2
T_i	= 353 K
T_f	= 323 K
T_{sf}	= 573 K (Carley, 1980)
χ_s	= 0.021
k_p	= 0.688 kcal/h·m·K (2.88 kJ/h·m·K) (Nottenburg, 1978)

TABLE 2. AUTOIGNITION MODEL VS. KINETIC MODEL

	Auto-ignition Model	Kinetic Models		
T_{sf}	573 K			
A_1	—	6.4×10^9 1/atm·h (6.31×10^7 1/kPa·h)	5.15×10^8 1/atm·h (5.08×10^6 1/kPa·h)	9.39×10^8 1/atm·h (9.26×10^6 1/kPa·h)
E	—	27 kcal/mol (113 kJ/mol)	23.2 kcal/mol (97.2 kJ/mol)	22.02 kcal/mol (92.19 kJ/mol)
V	0.097 m/h	0.095 m/h	0.0968 m/h	0.101 m/h
T_m	1,429 K	1,465 K	1,443 K	1,398 K
$\hat{x}$	0.292 m	0.34 m	0.35 m	0.38 m
η_s	0.195	0.145	0.130	0.095

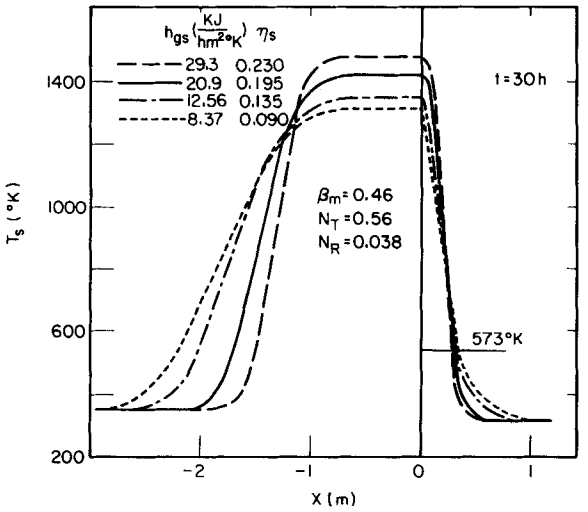

Figure 5. Influence of h_{gs} on the profile of the temperature of the solid.

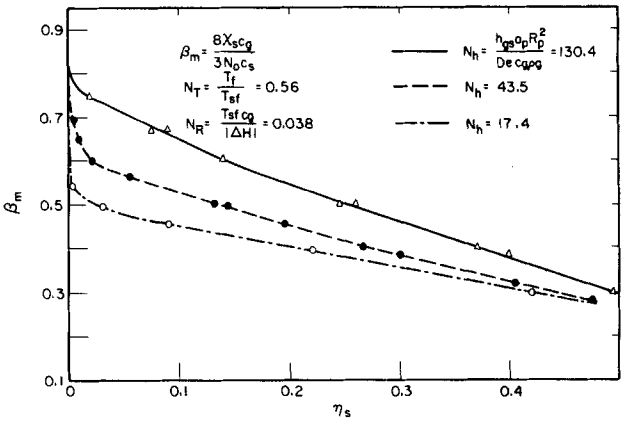

Figure 6. Correlation of calculated oxygen breakthroughs ($\beta < 1$).

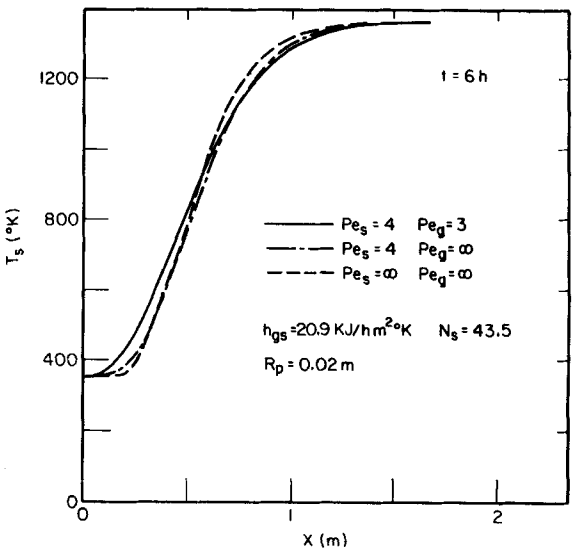

Figure 7. Solid temperature profile for the unsteady-state zone.

Oxygen Breakthrough

The breakthrough of oxygen or of carbon is extremely sensitive to changes of the temperature profile in the combustion zone. This is illustrated in Figure 5, which shows the influence of the heat transfer coefficient h_{gs} on the temperature profile. A decrease in h_{gs} reflects a decrease in the rate of heat transfer between the gas and the solid. As discussed in a previous section, this has the same effect as increasing the dispersion of heat in the x-direction and, therefore, gives rise to a more diffuse temperature profile.

It is noted that the decrease in h_{gs} also is accompanied by a decrease in the fraction of oxygen that escapes unburned, (η_s). This can be explained because a more diffuse temperature profile provides a longer combustion zone and, therefore, a larger conversion of oxygen.

The fraction of unburned oxygen or carbon must also depend on the rate of reaction between the carbon and oxygen in the combustion zone. Since the rate of this reaction is limited by the diffusion of oxygen through the burned shale, this points to the importance of the diffusion coefficient D_e in the denominator of N_h.

The strong influence of N_h on the breakthrough is illustrated in Figure 6 (for $\beta < 1$), where η_s is plotted as a function of β_m for different values of N_h. The same type behavior is also observed for carbon breakthrough for $\beta > 1$. It is to be noted that as β or β_m approaches one the oxygen or carbon breakthrough decreases to zero. This can be explained because as β or β_m approaches one, the maximum temperature in the combustion zone increases. An increase in the maximum temperature means that a larger portion of the front part of the temperature profile is in the combustion zone.

The calculations in Figure 7 were all done for a fixed value of the ratio of the downstream solid temperature to the ignition temperature, $N_T = T_f/T_{sf} = 0.56$. An increase in this ratio causes η_s to decrease. In fact, at $N_T \geq 1$ all of the bed is above the ignition temperature and the combustion will go to completion, $\eta_s = 0$.

The number $N_R = T_{sf}C_g/|\Delta H|$ used in our calculations is maintained constant and equal to 0.038. If the heat released by the exothermic combustion reaction, $|\Delta H|$, increases, the maximum temperature of the bed and the length of the combustion zone will increase. This means that the oxygen breakthrough, η_s, will decrease. Therefore a decrease of N_R is accompanied by a decrease of η_s.

Design Considerations

The main characteristics of the fully developed temperature profiles are calculated from very simple relations. From an overall heat balance the maximum temperature is given by

$$T_m = T_f + \frac{|\Delta H|\chi_s}{C_s|1-\beta|} \quad \text{for } \beta < 1 \tag{34}$$

and

$$T_m \simeq T_i + \frac{|\Delta H|\chi_s}{C_s|1-\beta|} \quad \text{for } \beta > 1 \tag{35}$$

As already indicated the velocity of the combustion zone is given by a mass balance as

$$V = \frac{3N_o \frac{\dot{m}_g}{A}(1-\eta_s)}{8\rho_s\chi_s(1-\epsilon)(1-\Psi_s)} \tag{2}$$

If Eq. 2 is substituted into the definition of β the following simple relation is obtained:

$$\beta = \frac{8\chi_s C_s}{3N_o C_s}\frac{1-\Psi_s}{1-\eta_s} = \beta_m \frac{1-\Psi_s}{1-\eta_s}. \tag{36}$$

Since, from Eq. 3, $V_{us} = \beta V$, an estimation of the length of the plateau region, L_p, is obtained

$$L_p = |1-\beta|Vt. \tag{37}$$

Equations 34, 35, 2 and 37 can be used to calculate the basic features of the temperature wave. All the quantities in these equations are given with the exception of the oxygen or carbon breakthrough (η_s or Ψ_s respectively). Consequently information of the type provided in Figure 6 is needed in order to complete the calculations.

Dispersion Effects

Estimates of the effective axial thermal dispersion coefficient for the solid, K_{es}, and for the gas, K_{eg}, can be obtained from the paper by Dixon (1979). An estimation of the axial diffusion of oxygen is obtained from the paper by Edwards (1968).

If a characteristic length, l, for the thermal wave is defined as

$$l = \frac{V\rho_s C_s|1-\beta|}{h_{gs}a_p} \tag{38}$$

the following dimensionless groups can be defined characterizing the dispersion of heat and the diffusion of oxygen:

For solid conduction: $Pe_s = \dfrac{lV\rho_s C_s(1-\epsilon)}{K_{es}}$

For gas conduction: $Pe_g = \dfrac{l\frac{\dot{m}_g}{A}C_g}{K_{eg}}$

For oxygen diffusion: $Pe_{ox} = \dfrac{l\frac{\dot{m}_g}{A}}{D_{ox}\rho_g\epsilon}$

The magnitude of these dimensionless groups suggests that for the conditions of the Lawrence Livermore Laboratory run S-11 axial conduction and diffusion effects are not negligible small.

In order to assess the effect of neglecting dispersion on the calculations presented in the previous sections, the following equations for the temperature of the gas and solid in the heating zone were considered:

$$\epsilon\rho_g C_g\frac{\partial T_g}{\partial t} = h_{gs}a_p(1-\epsilon)(T_s-T_g) - \frac{\dot{m}_g}{A}C_g\frac{\partial T_g}{\partial z} + K_{eg}\frac{\partial^2 T}{\partial z^2} \tag{39}$$

$$\rho_s C_s(1-\epsilon)\frac{\partial T_s}{\partial t} = -h_{gs}a_p(1-\epsilon)(T_s-T_g) + K_{es}\frac{\partial^2 T_g}{\partial z^2} \tag{40}$$

This system of equations was solved numerically using the method of lines (Carver et al., 1978). As shown in Figure 7 the inclusion of the effects of axial dispersion of heat causes the profile to be more diffuse.

As pointed out before a decrease in h_{gs} has the same effect as increasing the axial dispersion of heat. This is illustrated in Figure 8 where it is shown that the decrease of h_{gs} to a value between 2.5 kcal/h·m²·K (10.5 kJ/h·m²·K) and 3 kcal/h·m²·K (12.56 kJ/h·m²·K) has the same effect on the solid temperature profile as allowing K_{eg} and K_{es} to be nonzero. However, it should be recognized that the use of lower values for h_{gs} will mean that the calculated local rate of heat transfer between the solid and the gas will be much less. Therefore the calculated temperature difference, $T_s - T_g$, will be greater than what actually exists.

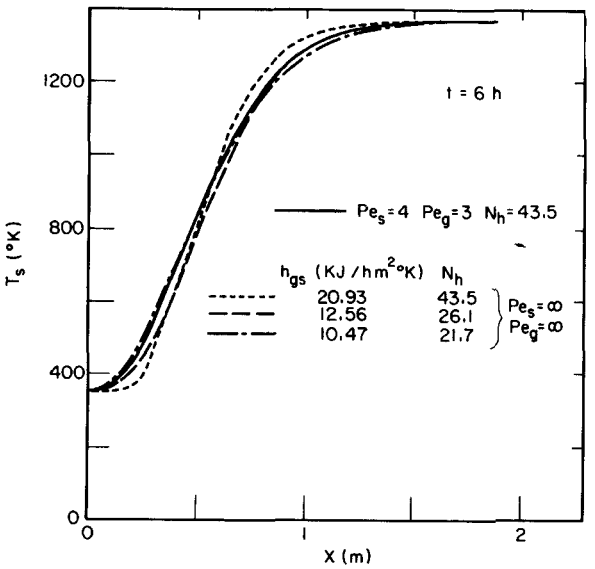

Figure 8. Solid temperature profile for the unsteady-state zone.

Since the inclusion of axial dispersion of heat in the solid causes a longer combustion zone it is expected that the resulting calculations would show a lower breakthrough of oxygen or carbon. However, the diffusion of oxygen would tend to have an opposite effect. This can be illustrated by considering the following equations for a steady state combustion zone:

$$-\frac{\dot{m}_g}{A}C_g\frac{dT_g}{dx} + h_{gs}a_p(1-\epsilon)(T_s-T_g) = 0 \tag{6}$$

$$V\rho_s C_s(1-\epsilon)\frac{dT_s}{dx} + K_{es}\frac{d^2T_s}{dx^2} - h_{gs}a_p(1-\epsilon)(T_s-T_g) - \Delta Hr(1-\epsilon) = 0 \tag{41}$$

$$-\frac{\dot{m}_g}{A}\frac{d\eta}{dx} + \epsilon D_{ox}\rho_g\frac{d^2\eta}{dx^2} - \frac{1-\epsilon}{N_o}r_{o_2} = 0 \tag{42}$$

$$V\rho_s\chi_s\frac{d\Psi}{dx} - r = 0 \tag{16}$$

$$r = \frac{3}{8}r_{o_2} \tag{17}$$

$$r = 0 \quad \text{for } T < T_{sf}$$

$$r = \frac{9N_o\rho_g}{8R_p}\frac{\eta}{\frac{R_p(\Psi^{-1/3}-1)}{De} + \frac{1}{K_g}} \quad \text{for } T > T_{sf} \tag{19}$$

Equation 42 can be integrated once using Eqs. 16 and 17 and the boundary conditions that $x = \hat{x}$, $\eta = \eta_s$, $\Psi = 1$, and $d\eta/dx = 0$:

$$\frac{d\eta}{dx} = \frac{\frac{\dot{m}_g}{A}}{\epsilon D_{ox}\rho_g}\left[(\eta-\eta_s) + \left(\frac{1-\eta_s}{1-\Psi_s}\right)(\Psi-1)\right] \tag{43}$$

Because the effect of oxygen diffusion is being included, the concentration of oxygen at the entry of the combustion zone, η_1, is not equal to the value at the bed entry, $\eta = 1$. Therefore η_1 at $x = 0$ is not known *a priori* and must be calculated from a mass balance (Danckwerts condition). The boundary conditions used in the solution of Eqs. 6, 41, 43, 16 and 19 are given as follows:

TABLE 3. DISPERSIVE VS. NONDISPERSIVE MODELS

	$\beta_m = 0.46$	$Pe_g = \infty$	$N_T = 0.56$	$N_R = 0.038$	
Pe_s	∞	4.3	4	∞	∞
Pe_{ox}	∞	∞	3.3	∞	∞
N_h	43.5	43.5	43.5	21.7	26.1
V (m/h)	0.097	0.110	0.107	0.108	0.106
T_m (K)	1,429	1,312	1,336	1,326	1,347
$\hat{x}$ (m)	0.292	0.350	0.355	0.340	0.330
η_s	0.195	0.100	0.125	0.115	0.135

For $\beta < 1$

$$x = 0 \quad \Psi = 0 \quad T_s = T_g = T_m$$
$$x = \hat{x} \quad \Psi = 1 \quad T_s = T_{sf}$$

For $\beta > 1$

$$x = \hat{x} \quad \eta = 0 \quad \Psi = 1 \quad T_s = T_g = T_m$$
$$x = 0 \quad T_s = T_{sf}$$

Note that in both cases $\hat{x}$ is unknown. These equations are solved numerically using an interative shooting method with two unknowns η_s and η_1 (Carnahan et al., 1976).

A summary of calculated results, using the values of Table 1, is given in Table 3. It is noted that the influence of the inclusion of the diffusion of oxygen and of the dispersion of heat in the solid greatly decreases the calculated breakthrough of oxygen. It also decreases the peak temperature of the solid and increases the length of the combustion zone.

It is of interest that the same effects can be obtained by decreasing h_{gs} so that N_h has a value between 21.7 and 26.1 (Table 3). This suggests the important parameters of the combustion zone can be calculated without including the effects of axial dispersion provided an adjusted value of h_{gs} is used.

The suggested method for doing this is to compare solutions of Eqs. 39 and 40 for the unsteady heating zone with and without dispersion effects. At present, the accuracy of this adjustment is not critical since, for the low Peclet region of an oil shale retort, the correct value of the heat transfer coefficient is known only within a factor of 10.

The dispersion of heat in the gas phase was neglected in our calculations. If we include this effect the gas temperature profile becomes more diffuse and the solid temperature profile more steep. Because we assume the reaction takes place in the solid phase and because the length of the combustion zone decreases, the oxygen or carbon breakthrough will be greater if we include the axial heat dispersion in the gas phase. Also the temperature difference between the gas and the solid will increase. This is only a qualitative result because of the difficulties of constructing a model to include the conductivity of the gas.

CONCLUDING REMARKS

The model presented for the combustion of a bed of carbon is valid only for the steady state temperature and concentration profiles that will develop after the combustion wave has moved through a considerable length of the bed. To our knowledge, experiments have not been performed that will allow direct verification of our results. However, recent numerical solutions of the unsteady Eqs. 4 and 5 carried out in our laboratory do reveal the establishment of the steady combustion waves discussed in this paper.

The significance of the results on oxygen and carbon breakthrough in the retorting of a bed of oil shale particles is not yet known. Other reactions occur in a shale retort which can consume oxygen and carbon. It is not anticipated that for $\beta < 1$ there will be a close correspondence between the calculated oxygen breakthrough and measured oxygen concentrations in the exit gases from a retort. However, the calculated oxygen breakthrough could be of significance in calculating yields in that they reveal that oxygen is available to consume fuel created by the kerogen decomposition. This would, therefore, suggest that very low values of β could be unfavorable for a retorting operation.

It should also be pointed out that the bed temperature predicted in this paper could be much larger than what would be observed in a shale oil retort, where the temperature rise is moderated by endothermic carbonate decompositions.

ACKNOWLEDGMENT

The authors gratefully acknowledge support for this work received from the Occidental Research Corp. and from the Shell Companies Foundation.

NOTATION

A_1 = pre-exponential factor in the rate equation for carbon combustion
A = area of bed section
a_p = ratio of the particle area to its volume
C_g = heat capacity of the gas
C_s = heat capacity of the solid
D_e = effective diffusion coefficient of oxygen through the burned shale
D_{ox} = effective axial diffusion coefficient of oxygen
E = activation energy for carbon combustion
h_{gs} = overall gas-solid heat transfer coefficient
K = effective dispersion coefficient
k_{eg} = effective axial conductivity of the gas
k_{es} = effective axial conductivity of the solid
K_f = gas conductivity
K_p = shale-oil rock conductivity
k_g = mass transfer coefficient through the gas film surrounding the particle
l = characteristic length, $\dfrac{V\rho_s C_s|1-\beta|}{h_{gs}a_p}$
L_P = length of plateau region
$\dot{m}_g$ = mass flux of the gas
N_o = weight fraction of oxygen in the gas in the entry section
R = universal gas constant
R_p = particle radius
r = rate of carbon consumption
r_{o_2} = rate of oxygen consumption
T = mean temperature, $\dfrac{T_s + T_g}{2}$
T_f = initial temperature of the carbon bed
T_g = gas temperature
T_i = gas temperature at the entry section
T_m = plateau region temperature $T_s = T_g = T_m$
T_s = solid temperature
T_{sf} = auto-ignition temperature of carbon
t = time
V = combustion front velocity
V_{us} = unsteady-state heating zone velocity
x = length of the bed
$\hat{x}$ = length of the combustion zone

Dimensionless Parameters

$$N_h = \frac{h_{gs}a_p}{\dfrac{De}{R_p^2}C_g\rho_g} \qquad Pe_g = \frac{l\dfrac{\dot{m}_g}{A}C_g}{K_{eg}}$$

$$N_T = \frac{T_f}{T_{sf}} \qquad Pe_s = \frac{lV\rho_s C_s(1-\epsilon)}{K_{es}}$$

$$N_R = \frac{T_{sf}C_g}{|\Delta H|} \qquad Pe_{ox} = \frac{\dfrac{\dot{m}_g}{A}l}{D_{ox}\rho_g\epsilon}$$

Greek Letters

β = ratio of heat capacity rates, $\dfrac{\dfrac{\dot{m}_g}{A}C_g}{V\rho_s C_s(1-\epsilon)}$

β_m = modified beta, $\frac{8\chi_s C_g}{3N_o C_s}$

ΔH = heat of reaction

ϵ = void fraction

η = fraction of oxygen remaining

η_1 = fraction of oxygen remaining at the entry of the bed

η_s = fraction of oxygen remaining at the end of the bed (oxygen breakthrough)

μ_g = gas viscosity

χ_s = weight fraction of carbon in the pyrolyzed shale

Ψ = fraction of carbon remaining

Ψ_s = carbon breakthrough

LITERATURE CITED

Baer, A. D., and C. A. Dahl, "A Simple Semisteady-State Model of the Combustion Retort," *in situ*, **4** (1), 79 (1980).

Braun, R. L., "Results of Computer Simulation of *in situ* Oil Shale Retorting," *in situ*, **3**, (3), 173 (1979).

Campbell, J. H., and M. L. Gregg, "A Back of the Envelope Method for Predicting Thermal-Front Velocities During Oil-Shale Retorting," Lawrence Livermore Laboratory, Livermore, CA, UCID-18325 (1979).

Carley, J. F., "Spontaneous Ignition in Preheated Beds of Spent Oil Shale," *in situ*, **4** (4), 293 (1980).

Carnahan, B., H. A. Luther, and J. O. Wilkes, "Applied Numerical Methods," John Wiley and Sons, 407 (1976).

Carslaw, H. S., and J. C. Jaeger, "Conduction of Heat in Solids," Oxford Press, London, 398 (1959).

Carver, M. B., "The Forsim VI Simulation Package for the Automated Solution of Arbitrarily Defined Partial and/or Ordinary Differential Equation Systems," Chalk River Nuclear Laboratory, Ontario, Canada (1978).

DeAcetis, J., and C. Thodes, "Mass and Heat Transfer in Flow of Gases through Spherical Packings," *Ind. Eng. Chem.*, **52**, 1003 (1960).

Dixon, G. A., and D. L. Cresswell, "Theoretical Prediction of Effective Heat Transfer Parameters in Packed Beds, *AIChE J.*, **25** (4), 663 (1979).

Dockter, L., and T. F. Turner, "Combustion Rates for Oil Shale Carbonaceous Residue," *in situ*, **2** (3), 197 (1978).

Edwards, M. F., and J. F. Richardson, "Gas Dispersion in Packed Beds," *Chem. Eng. Sci.*, **23** 109 (1968).

Fausett, D. W., "A Mathematical Model of an Oil Shale Retort," *Colorado School of Mines Quart.*, **70** (3), 273 (1975).

Hougen, O. A., and W. R. Marshall, "Adsorption from a Fluid Stream Flowing through a Stationary Granular Bed," *Chem. Eng. Prog.*, **43** (4), 197 (1947).

Mallon, R. C., and R. L. Braun, "Reactivity of Oil Shale Carbonaceous Residue with Oxygen and Carbon Dioxide," *Colorado School of Mines Quart.*, **71** (4), 309 (1976).

Nottenburg, R., et al., "Meaasurement of Thermal Conductivity of Green River Oil Shales by a Thermal Comparator Technique," *Fuel*, **57**, 791 (1978).

Perry and Chilton, *Chemical Engineers Handbook*, McGraw-Hill, 5th ed. (1969).

Shih, S. M., and H. Y. Sohn, "A Mathematical Model for the Retorting of a Large Block of Oil Shale: Effect of the Internal Temperature Gradient," *Fuel*, **57**, 622 (1978).

Sohn, H. Y., "The Law of Additive Reaction Times in Fluid-Solid Reactions," *Met. Trans. B.*, **9B**, 89 (1978).

Sohn, H. Y., and K. S. Kim, "Intrinsic Kinetics of the Reaction between Oxygen and Carbonaceous Residue in Retorted Oil Shale," *Ind. Eng. Chem. Process Des. Dev.*, **19** (4), 550 (1980).

Soni, Y., and W. Thomson, "Oxidation Kinetics of Oil Shale Char," *Ind. Eng. Chem. Process Des. Dev.*, **18** (4), 661 (1979).

Thomson, W. J., "Oil Shale Char Reactions," *Chem. Eng. Ed.*, **15** (4), 184 (1981).

Yoon, H., J. Wei, and M. Denn, "A Model for Moving Bed Coal Gasification Reactors," *AIChE J.*, **24** (5), 885 (1978).

Manuscript received January 4, 1982; revision received May 18, and accepted June 18, 1982.